Spin-dependent electrical hole extraction from low doped p-Si via the interface states in a Fe_3Si/p-Si structure

A.S. Tarasov[1,2], A.V. Lukyanenko[1,2], M.V. Rautskii[1], I.A. Bondarev[1,2*], D.A. Smolyakov[1], I.A. Tarasov[1], I.A. Yakovlev[1], S.N. Varnakov[1], S.G. Ovchinnikov[1,2], F.A. Baron[1] and N.V. Volkov[1]

[1] Kirensky Institute of Physics, Federal Research Center KSC SB RAS, Krasnoyarsk 660036, Russia
[2] Institute of Engineering Physics and Radio Electronics, Siberian Federal University, Krasnoyarsk 660041, Russia

[*]e-mail: bia@iph.krasn.ru

Abstract. Spin accumulation effect in Fe_3Si/p-Si structure with low boron doped silicon substrate was found. Calculated spin lifetimes are comparable with results reported earlier but for the structures with highly doped semiconductors (SC) with or without tunnel barrier introduced between SC and ferromagnet (FM). Electrical characterization of prepared Fe_3Si/p-Si diode allowed determining possible reasons of pronounced spin signal. Analysis of the forward bias I-V curve revealed Schottky barrier at the Fe_3Si/p-Si interface with a height of $\phi_{Bp} = 0.57eV$. Then, using the impedance spectroscopy, we observed interface states localized in the band gap of silicon with energy of E_{LS} = 40 meV. Such states most probably cause the observed spin signal. We believe that in our experiment spin-dependent hole extraction was performed via the interface states resulting in the minority spin accumulation in silicon valence band. Observed effect paves the way to the development of different spintronic devices based on FM/SC structure without dielectric tunneling barrier.

Introduction

Addition of spin transport to CMOS and SOI devices should lead to a new generation of devices with the non-volatile memory properties, high processing speed and high integration density [1, 2, 3, 4, 5]. At present, there is a large number of works on spin-dependent transport phenomena in different SC-based structures [6]. Moreover, there have been several reports on spin transistor working prototypes operated by magnetic or electric field or by optical methods [7, 8, 9, 10]. Carrier spin injection into a semiconductor (SC) is the first necessary condition to introduce spin degree of freedom into traditional electronics. Spin injection was demonstrated in Si [11, 12], Ge [13, 14], GaAs [15, 16] and other semiconductors [17, 18] with various doping levels and types using different ferromagnetic materials as injectors and dielectric films as tunneling barriers. Large scientific interest is paid to spin injectors based on ferromagnetic (FM) Heusler alloys with high spin polarization, like Fe_3Si, Co_2FeSi, Fe_2MnSi, Co_2FeAl, since they can be epitaxially grown on various semiconducting substrates [19, 20, 21, 22, 23, 24]. In most of the experiments on spin injection, in order to resolve well known problem of conductivity mismatch 3 basic approaches are used, together or separately: (i) introduction of tunnel insulator layer between FM metal and SC [11], (ii) heavily or degenerately doped SC wafers (10^{18} cm^{-3} carrier concentration and higher) [11, 12] and (iii) δ- doped high carrier concentration sublayer on SC substrate surface [15, 19]. The first method directly forms a tunnel barrier, the next two - reduce the depletion region width in SC to increase the tunneling rate through Schottky barrier. One of the few works devoted to studying the Schottky barrier role in spin injection effectiveness demonstrated the possibility of spin injection into p-type silicon with doping density as low as 10^{15} cm^{-3}, but through tunnel SiO_2 layer [25]. It was shown regardless of barrier width the localized interface states contribute to the spin-polarized electron tunneling current.

Furthermore, recent work of Rortais *et al.* [26] revealed the influence of defects on electrical spin injection into silicon and germanium, and showed that defects in dielectric layer have no significant contribution to the spin signal, large spin signal magnitude is rather related to the presence of localized states at the MgO/Si interface. One may assume that localized interface states on the Si side can play an important role in the spin transport process in FM/insulator/SC structures. Therefore the effect of localized states and paramagnetic centers in Si requires further investigation. We believe that FM/SC structures and devices based on low doped wafers lack enough attention from the spin device research community. To the best of our knowledge there are no reports on spin accumulation effect measurements in the low doped silicon FM/SC structure, especially of those that utilize 3- terminal Hanle (3-T) [3] or nonlocal technique [27]. By low doping we mean lower than 10^{18} cm^{-3} carriers concentration in semiconductor wafer or in δ- doped layer.

In this work, we show the spin accumulation effect in Fe_3Si/p-Si FM/SC structure processed using low boron doped wafer ($p = 2 \times 10^{15}$ cm^{-3}). Most likely the spin signal observed is due to the localized interface states, which were experimentally detected using the impedance spectroscopy (IS).

Experimental details

A 50-nm-thick Fe_3Si epitaxial layer was grown at room temperature on moderately doped 350 μm-thick p-Si(111) substrate with boron concentration 2×10^{15} cm^{-3} (resistivity $\rho = 7$ Ω·cm) by molecular beam epitaxy (MBE) in ultrahigh vacuum conditions (UHV) using specialized MBE system described elsewhere [28]. Details of the epitaxial iron silicide synthesis technology with the DO3 structure were described previously [29,30]. The evolution of the RHEED pattern during the Fe_3Si epitaxial film growth is represented in Figure 1. RHEED pattern corresponded to the deposition time (t = 0 min) clearly shows the presence of Si(111)7x7 surface reconstruction. After 1 minute of the deposition process (0.8 ML) the 7x7 reconstruction is absent while three spot reflections on (01), (00), (01) streaks are still recognizable. This stage may correspond to the growth stage when the sample surface consists of the flat growing islands of Fe_3Si phase and clear Si(111)1x1 surface. The streak intensity increase and their broadening is easily noticeable at t = 3 min (2.5 ML) due to increased proportion of growing silicide islands. The spot reflections disappear at value of 4.2 ML and the RHEED pattern does not have other different reflections further. One can consider the Fe_3Si epitaxial thin film growth as the 3D island growth mode since at nominal thickness higher than 1ML the Si(111)1x1 reflection may be still noticed. The continuous Fe_3Si epitaxial film is appeared to be at 5 nm according to our previous research [31]. Thus, interfacial layer may contain higher quantity of structural defects formed during the coalescence of 3D islands than the rest of the film volume. This was confirmed earlier by examination of an Fe_3Si epitaxial film with Rutherford backscattering spectrometry (RBS) channelling measurements [30]. Namely, the minimum yield χ_{min} shows increased values for the interfacial region Fe_3Si/Si in comparison with the main film body. Moreover, the interfacial region is usually enriched with silicon atoms due to silicon atom diffusion from the silicon substrate at elevated temperatures [32]. Thus, one may expect that the interfacial layer can demonstrate slightly different properties with respect to the main film volume due to changes in the chemical composition and chemical order [33,34].

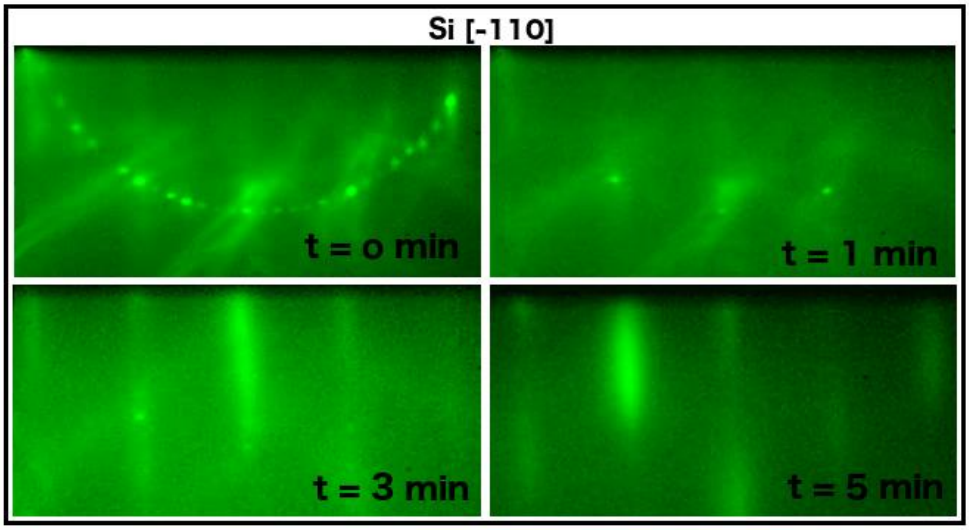

Fig.1 Evolution of experimental RHEED pattern along Si[-110] direction of Si(111) surface during the Fe_3Si epitaxial film growth.

In order to confirm epitaxial orientation relationship (OR) of Fe_3Si/Si heterostrucuture the RHEED pattern of as-grown Fe_3Si epitaxial thin film (Fig. 2 (upper row)) was simulated with the kinematical approach (Fig. 2 (lower row)), considering single electron scattering events at the surface [35]. The OR obtained is $Fe_3Si(111)[1\text{-}21] \parallel Si(111)[11\text{-}2]$, which is consistent with our previous results [30,36]. Moreover, the RHEED simulation approach allows us additionally to carry out an estimation of the surface roughness. It indicates the formation of islands with the length of 3 nm and three $Fe_3Si(111)$ monolayers high (~1 nm) and laying on the $Fe_3Si(111)$ surface with the coverage of 0.3 ML. The typical average roughness (~1 nm) of the Fe3Si films measured by atomic force microscopy [30] is in agreement with the simulation results.

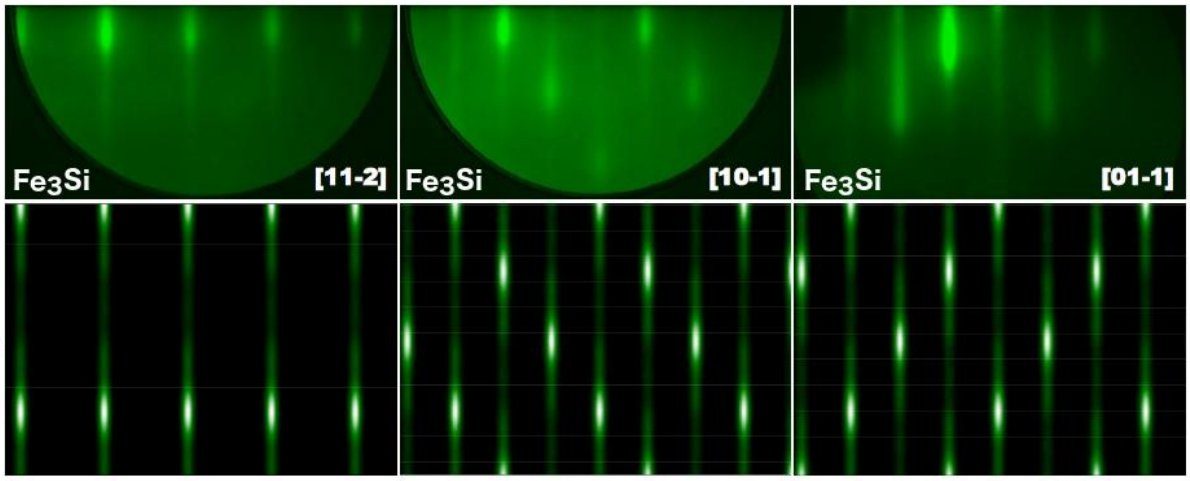

Fig.2 Upper row corresponds to experimental RHEED pattern along [11-2], [10-1] and [01-1] directions of $Fe_3Si(111)$ surface after the growth. Lower row – simulated RHEED patterns of Fe_3Si surface at the same beam directions.

Polar (out-of-plane) and azimuthal (in-plane) angular dependences (at 5° angular resolution) of ferromagnetic resonance (FMR) spectra measured with the X-band (9.7 GHz) spectrometer ELEXSYS E580 (Bruker, Germany). Figure 3(a) represents the polar angular dependences of the resonance field H_R that is defined as the H value where the derivative of P with respect to H is equal to zero: $H_R = H|_{dP/dH=0}$. Here, P is the absorbed microwave power. The maximum of H_R (14580 Oe) corresponds to the hard magnetization axis and observed when the external magnetic

field is normal to the film plane (θ= 0). The minimum of H_R (857 Oe) corresponds to the easy axis and observed when the external magnetic field is directed within the film plane. This behavior indicates that the magnetic properties of the films are determined by the shape anisotropy. Furthermore, the azimuthal angular dependence of the resonance field H_R (Fig. 3(b)) demonstrates the presence of crystalline anisotropy in the plane of the film. The saturation magnetization calculated from the analysis of the angular dependences of FMR resonance field amounts to 1150emu/cm^3, which is close to the maximum for bulk single crystal [37] and epitaxial thin films [38,39,40]. The large saturation magnetization in combination with a small FMR linewidth (~17 Oe in-plane geometry) indicates the high quality of the Fe_3Si film.

For 3-T measurements in Fe_3Si/Si structure, 3-terminal planar micro-scale device was fabricated (Fig. 3(c)) using conventional photolithography process and wet chemical etching in HF: HNO_3: H_2O = 1: 2: 400 [30]. The distance between contact № 2 and contact № 3 is 10 μm. To study the Fe_3Si/Si interface electric properties, a diode was fabricated with ohmic contact on substrate backside (Fig. 3(d)), for which the measurements of *I-V* characteristics were performed as well as the temperature and frequency dependences of the real (Re |Z|) and imaginary (Im |Z|) parts of impedance. Studies of charge transport were performed at cryogenic probe station Lakeshore EMPX-HF 2 and homebuilt facility based on a helium cryostat and electromagnet [41,42] using Keithley 2634b SourceMeter and Agilent E4980A for dc and ac measurements, respectively, in the temperature range from 4.2 K to 300 K.

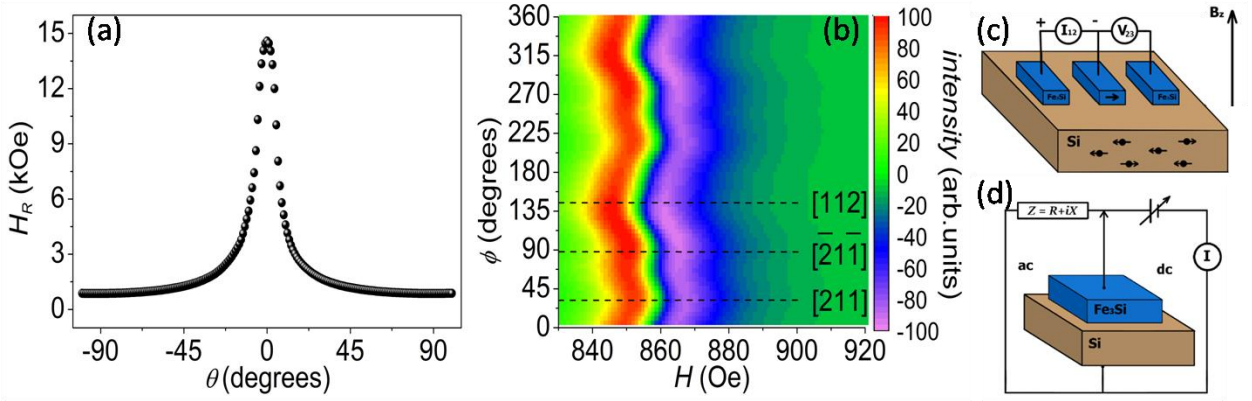

Fig.3 (a) The polar angular dependences of the resonance field H_R (out-of-plane geometry). (b) Amplitude map of azimuthal angular dependence FMR spectra (in-plane geometry). Dashed lines show the crystal orientations [112], [-21-1] and [211]. Experimental schemes and sketches of (c) 3-terminal planar microdevice for studying Hanle effect and (d) Schottky diode for electrical characterization.

Result and Discussion

Firstly, magnetic field dependences of voltage signal ΔV_{23} were measured at bias current I_{12} = 500 μA using experimental geometry shown in Fig. 3(c). Curves for different temperatures behave similarly and have a Lorentzian shape (Fig. 4). It indicates the occurrence of spin accumulation under the contact № 2 according to the 3-T method. Injected carriers polarization is parallel to the magnetization direction of the ferromagnetic contacts and lies in the sample plane. Out of plane magnetic field causes spin precession that results in spin accumulation suppression. Note that in the experiment, bias current I_{12} was positive, i.e., the contact № 2 was under negative bias. That means that the device works in a hole extraction regime. Consequently, spin accumulation is caused by spin-dependent hole extraction from silicon to Fe_3Si. Moreover, we observed spin signal only in the perpendicular magnetic field (as shown in Fig. 3(c)), i.e., direct Hanle effect. At the same time inverted Hanle effect [43], which is measured when a

magnetic field is applied in the film plane, was not found in our structure. This effect appears in structures with rough interface and is related to spin dephasing due to an inhomogeneous magnetostatic field near a ferromagnetic interface. In other words inverted Hanle effect must be observed when a fraction of accumulated spins is oriented at certain angle with respect to the structure plane due to the interface roughness. In this case the in-plane magnetic field should enhance the spin accumulation. Since such effect has not been observed one may assume that Fe_3Si film is very smooth.

Using the expression $\Delta V(H)= \Delta V\ (0)/(1+(\omega_L \tau_s)^2)$ for 3-T Hanle signal [11, 26] we fitted the experimental data by the Lorentzian function (Fig. 4). The extracted half-width of the fitting curve in its half-max ΔB allows calculating spin lifetime $\tau_s= 1/\omega_L=h/2\pi g_h \mu_B \Delta B$, where g_h is the Lande g-factor of holes (g_h=2). For our devices experimental curves fitting yeilds the following values: τ_s = 145 ps, 191 ps, 268 ps, and 124 ps, for T = 300 K, 200 K, 120 K, and 100 K, respectively. As can be seen from the inset of figure 4 temperature dependence of spin lifetime has nonmonotonic behavior. Initially with decreasing temperature from 300 K to 120 K τ_s is increasing. Further cooling below 120 K leads to the decrease of τ_s. Furthermore, at 80 K spin signal disappears and, consequently spin lifetime can't be extracted from experimental curve. At this stage of research it is difficult to give a detailed explanation or suggest mechanisms responsible for the observed temperature dependence, only some speculations can be made. Papers [44,45] provide similar features of spin lifetime observed in n-Si and n-Ge. Ishikawa *et al.* [45] shows that the temperature-dependent τ_s in Si layers originates from the temperature-dependent mobility μ and diffusion length D. Such explanation may account for our results at temperatures above 120 K. Based on *Sze* [46] both μ and D parameters in p-Si should increase when cooling below the room temperature, consequently τ_s should also increase. However, within the framework of this simple model, the low-temperature behavior of τ_s cannot be understood. Also this effect cannot be related to any peculiar feature in temperature dependence of specific resistance of Fe_3Si, which gradually decreases from room temperature down to liquid helium. This complex behavior could be related to the carrier freeze out in low-doped Si below 120 K [46] resulting in exponential drop of the holes concentration at low temperatures. Nevertheless obtained values of the spin lifetime are comparable with other reported results for silicon-based structures probed by 3-T measurements. For example, for a structure with an epitaxial MgO(001) tunnel barrier and Fe(001) electrode τ_s in highly doped p-Si is 133 ps [47]. Previously reported [43] spin lifetime values in highly doped p-Si with Al_2O_3 tunnel barrier and different ferromagnetic electrodes were 60 ps, 110 ps and 270 ps for Fe, Co, and $Ni_{80}Fe_{20}$ electrodes, respectively. Another paper [19] reports τ_s = 470 ps in the FM/SC structure Fe_3Si/n-Si with δ-doped layer with narrow width Schottky barrier. However, it is important to note that in our case the spin injection occurred into the low doped wafer with relatively high resistivity (p = 2×10^{15} cm^{-3}, ρ = 7 Ω·cm). Moreover, our Fe_3Si/p-Si structure did not contain a tunnel insulator layer between FM and SC. According to standard spin diffusion model [48], those two circumstances create mismatch conductivity problem which should have strongly reduced the spin signal. So, let us explore the reasons why the spin accumulation effect was quite pronounced in our device.

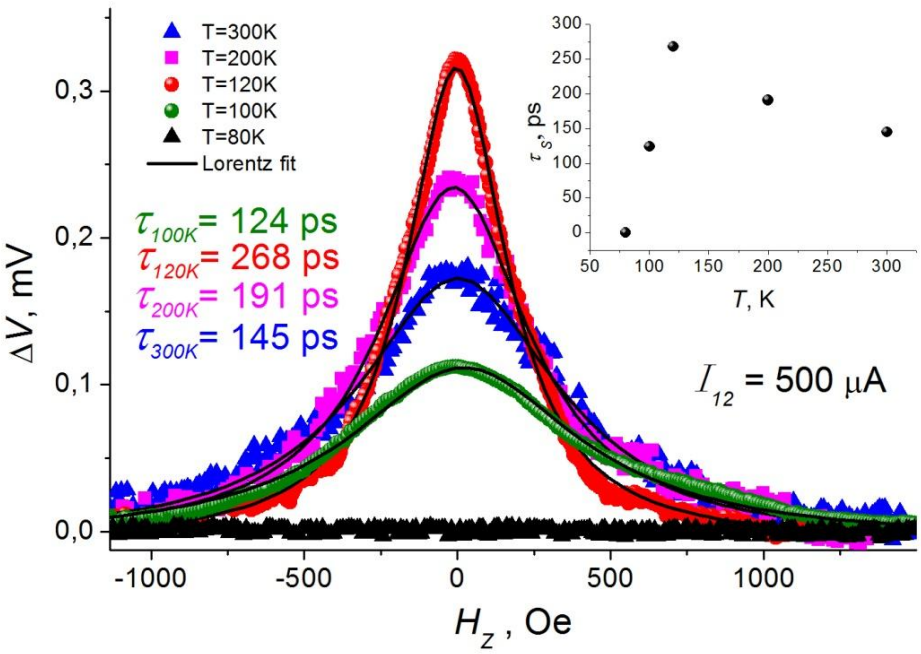

Fig.4 Hanle curves for Fe_3Si/p-Si device at I_{12} = +500 μA and temperatures of 300K, 200K and 120K (symbols) and Lorentzian fits (solid lines)

First of all, for spin injection into high resistive Si interface resistance should be significant. For FM/SC structure, the Schottky barrier could provide such high such resistance. We measured the *I-V* characteristics of specially prepared Fe_3Si/p-Si diode and found that the curves demonstrate rectifying behavior Fig. 5(a), which indicates the presence of the Schottky barrier. Indeed, analysis of the forward bias I-V curve by Cheung's method [49] revealed Schottky barrier at Fe_3Si/p-Si interface, with height $\phi_{Bp} = 0.57eV$. However, for silicon with 2×10^{15} cm^{-3} doping the depletion region width is about 700 nm [50], and such a barruer has very small tunneling rate. In this case, the charge transport may occur due to the charge transfer over the barrier by thermionic emission. Therefore, the presence of the Schottky barrier in our structure can hardly be the sole cause of the spin-dependent transport effect.

The work of Dankert *et al.* [25] reported efficient spin injection into silicon through 736-nm-wide Schottky barrier and tunneling SiO_2 layer simultaneously. Authors considered the mechanism of spin injection by tunneling via interface states, the model of which was suggested earlier [51]. However, there were no attempts to detect such states, for example, by optical or electrical spectroscopy techniques. Assuming that in our structure there might be various surface and interface states that are most likely caused the observed spin signal, we tried to detect them using impedance spectroscopy (IS) [52,53,54]. By this technique one could measure the thermal emission rate in the space-charge region located very close to the crossing point of the Fermi level with the energy level of states localized near insulator/semiconductor interface. Search of the crossing point is carried out by temperature scanning during IS experiment that induce movement of Fermi level within forbidden band.

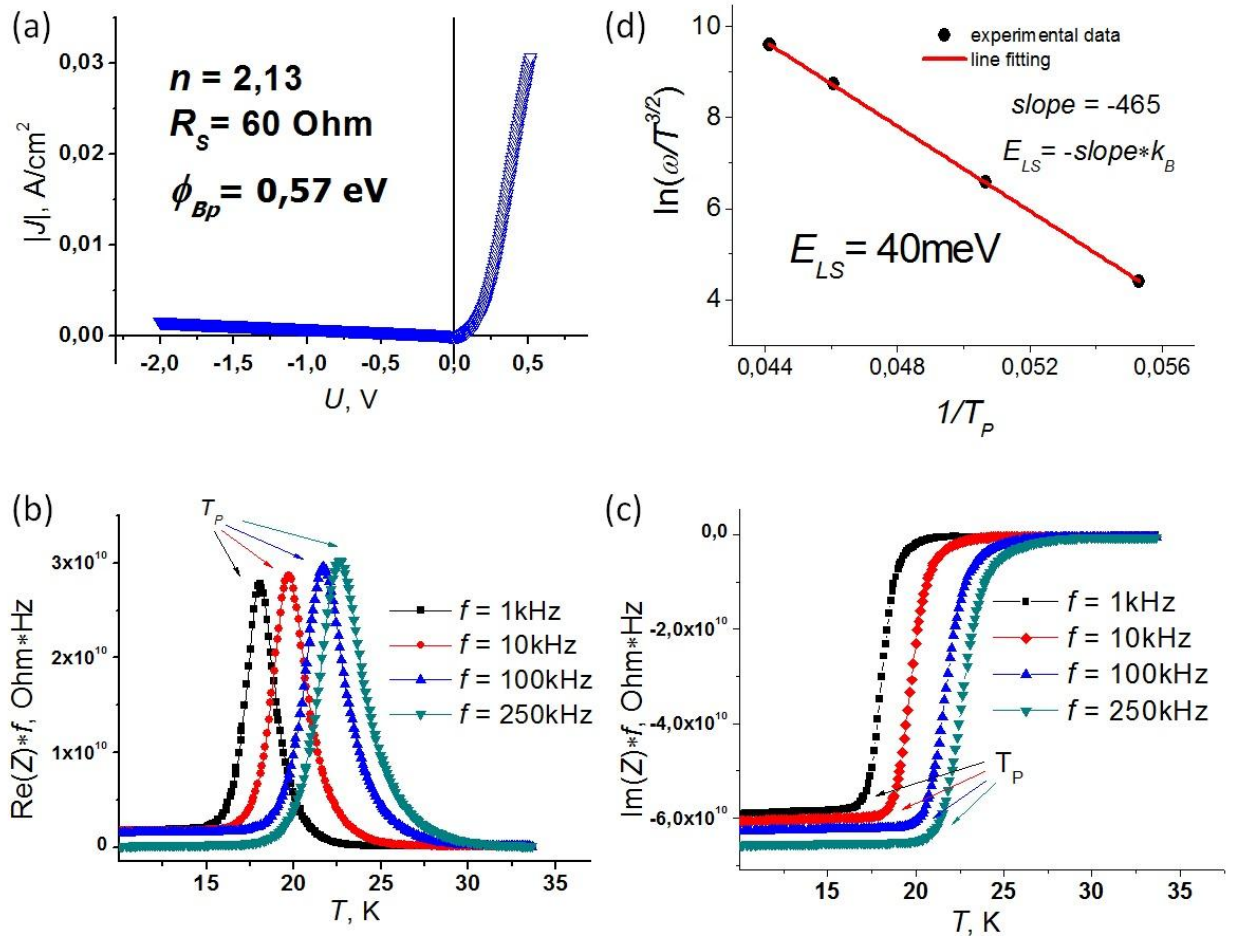

Fig.5(a) *I–V* curve of the Fe_3Si/p-Si Schottky diode at 295 K. Temperature dependences of normalized (b) active and (c) reactive resistances at different frequencies. (d) $ln(\omega/T_P^{3/2})$ versus $1/T_P$ plot allows calculating energy of localized states E_{LS}.

For the same Fe_3Si/p-Si diode temperature dependences of real and imaginary parts of impedance were measured (Fig. 5(b) and Fig. 5(c)). At low temperatures, we observed sharp peak on the resistance curve and the peak temperature position T_P is frequency-dependent. This indicates the presence of a thermally activated energy state. This state charge-discharges under the action of ac voltage bringing up peaks and step features on the frequency and temperature plots of ac resistance, reactance, admittance or impedance. One can estimate the state energy using the following expression for the recharging rate: $\langle\omega\rangle = 2C\ N_V \exp\left(-E_{LS}/k_BT\right)\beta^{-1}$ [52]. Here $\omega=2\pi f$ is the angular frequency of applied ac voltage, C – capture coefficient, k_B – Boltzman constant, β – degeneracy factor. Since valence-band density of states $N_V(T)\sim T^{3/2}$ one can extract the energy of localized states E_{LS} from the slope of $ln(\omega/T_P^{3/2})$ versus $1/T_P$. We obtained E_{LS} = 40 meV for the extracted value of T_P observed at frequencies from 1 kHz to 250 kHz (Fig. 5(d)). Such low energy means that detected states can participate in dc transport processes even at room temperature. Assuming the presence of $\phi_{Bp} = 0.57eV$ Schottky barrier and localized interface states in our structure, we can construct the energy band diagram and propose a scheme of spin-polarized holes transport (Fig. 6). As mentioned above, contact № 2 was under negative bias (Fig. 3(c)), i.e. our device worked in spin extraction regime. Holes from the valence band tunnel via localized states into Fe_3Si electrode. Tunneling probability of spin polarized carriers depends on density of states (DOS) of corresponding spin subbands $D\uparrow(E_F)$ and $D\downarrow(E_F)$ in ferromagnetic electrode. Initially both spin polarizations of holes in silicon

valence band have equal DOS. However, since in Fe_3Si electrode spin up $D\uparrow(E_F)$ and spin down $D\downarrow(E_F)$ subbands DOS are different the hole transport from Si to Fe_3Si become spin polarized. If Fe_3Si is spin up polarized, i.e. $D\uparrow(E_F) - D\downarrow(E_F) > 0$, then the spin up transport channel prevails. We believe that as a result of the spin up polarized holes extraction there occurs the spin accumulation of holes with spin down direction in the silicon valence band, i.e. minority spin accumulation. This process is highlighted in Fig. 6. In reality the spin down holes also take part in the transport but probability of this process is much lower. Worth mentioning is the possibility of energy levels splitting of the localized states. Thus formed spin subbands would also have different tunneling probabilities. Another important requirement for the two step tunneling to take place is availability of unoccupied localized states at interface. We believe that the low values of energy E_{LS} extracted from our IS data is a strong indication that, indeed, such sates are empty within the temperature range in our 3T-Hanle experiment. Unfortunately at this stage of our research studies it is hard to elucidate the nature of these states. Perhaps they are formed at the initial stage of the film growth process.

Another possible reason for the sharp spin signal is extremely high spin polarization of the ferromagnetic contact. On the one hand, the spin polarization of ideal structurally and chemically ordered DO_3 Fe_3Si is about 50% [55]. On the other hand, Karel *et al.* [34] calculated DOS and theoretically showed that the spin polarization can change from -12% to 77% due to variation of the chemical order in the $Fe_{0.65}Si_{0.35}$ compound. The strong dependence of Fe magnetic moment on the nearest-neighbor environment of iron in Fe_3Si and Fe_xSi_{1-x} compounds was shown in work of Zamkova *et al.* [56]. Therefore, it can be assumed that Fe_3Si in our structure has an imperfect chemical order DO_3 (this is also indicated by XRD data [36]) which leads to an increase of the spin polarization above 50%. However the 100% spin polarization condition is likely not satisfied in our structure and it is needed to circumvent the conductivity mismatch problem allowing barrier-free diffusive spin transport. Still using the proposed scheme of the interface states-assisted tunneling in conjunction with Fe_3Si highly spin polarized electrode may deliver higher spin injection efficiency than other structures containing simple 3d ferromagnetic metals like Fe or Co.

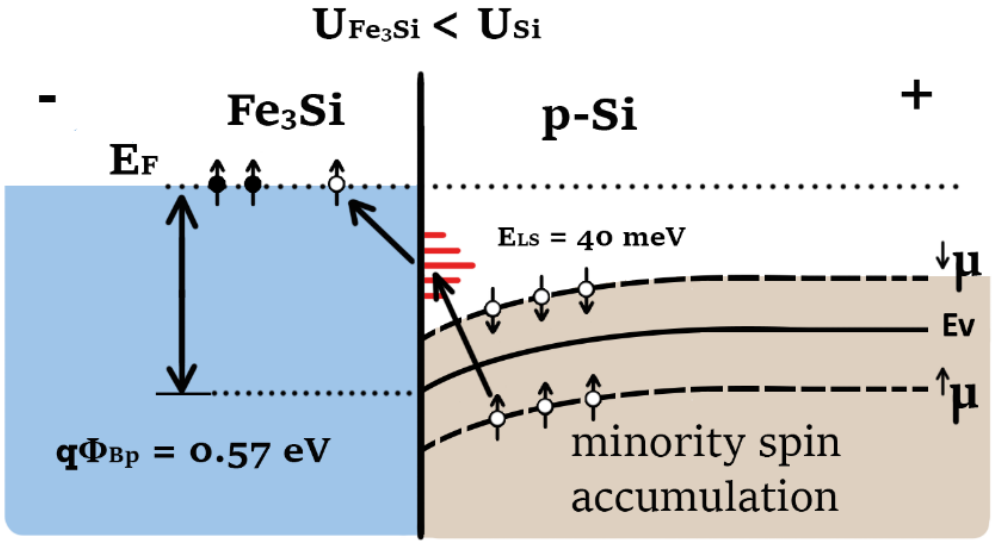

Fig.6 Schematic energy-band diagram depicting spin-polarized holes transport through the Fe_3Si/p-Si junction via localized interface states assisted tunneling.

Conclusions

Spin accumulation in low doped p-Si with epitaxial Fe_3Si film was studied using 3-T Hanle method. Room temperature spin lifetime τ_s=145 ps was extracted from the voltage versus magnetic field Lorentzian curves. Obtained data is in a good agreement with other reported results for silicon-based devices. However, according to the standard spin diffusion model, our structure should not demonstrate spin accumulation effect due to the high resistivity of the substrate, which is the reason why most of the spin injection experiments with the SC transport use channel with high carrier concentration. We proposed several reasons for explaining the experimental data. Most probably, the pronounced spin signal was due to the presence of localized interface states at the Fe_3Si/Si interface. This suggestion is supported by impedance spectroscopy (IS) measurements. Within the framework of our model IS revealed the interface states with energy E_{IS} = 40 meV above the valence band edge in silicon. Thus, we suggest that spin-dependent transport between Fe_3Si and p-Si was realized via the interface states, which led to minority spin accumulation in silicon valance band. Observed at room temperature this giant spin accumulation phenomenon indicates that it may become possible to create spintronic devices based on FM/SC structures without dielectric tunneling barrier. We believe that our experimental findings may help develop a deeper understanding of spin transport phenomena in FM/SC structures.

Acknowledgments

The reported study was funded by Russian Foundation for Basic Research, Government of Krasnoyarsk Territory, Krasnoyarsk Region Science and Technology Support Fund by project № 18-42-243022 and supported in part by the Russian Foundation for Basic Research by project no. 18-32-00035. The work was partially supported by the Ministry of Education and Science of the Russian Federation and by Siberian Branch of the Russian Academy of Sciences (Project II.8.70) and Fundamental research program of the Presidium of the RAS no. 32 «Nanostructures: physics, chemistry, biology, basics of technologies».

[1] Sato, K., Saitoh, E., Willoughby, A., Capper, P., & Kasap, S. (Eds.). (2015). *Spintronics for next generation innovative devices*. John Wiley & Sons, Chap.10.
[2] D. E. Nikonov, I. A. Young, Overview of Beyond-CMOS Devices and a Uniform Methodology for Their Benchmarking Proceedings of the IEEE V: 101, I: 12, (2013).
[3] Jansen, R., Dash, S. P., Sharma, S., & Min, B. C. (2012). Silicon spintronics with ferromagnetic tunnel devices. *Semiconductor Science and Technology*, *27*(8), 083001.
[4] Žutić, I., Fabian, J., & Sarma, S. D. (2004). Spintronics: Fundamentals and applications. *Reviews of modern physics*, *76*(2), 323.
[5] Žutić, I., Fabian, J., & Erwin, S. C. (2006). Spin injection and detection in silicon. *Physical review letters*, *97*(2), 026602.
[6] Txoperena, O., & Casanova, F. (2016). Spin injection and local magnetoresistance effects in three-terminal devices. *Journal of Physics D: Applied Physics*, *49*(13), 133001.
[7] Chuang, P., Ho, S.C., Smith, L.W., Sfigakis, F., Pepper, M., Chen, C.H., Fan, J.C., Griffiths, J.P., Farrer, I., Beere, H.E., Jones, G.A.C., Ritchie, D.A., Chen, T.M. (2015) All-electric all-semiconductor spin field-effect transistors. *Nat. Nanotechnol.* 10, 35–39
[8] Koo, H. C., Kwon, J. H., Eom, J., Chang, J., Han, S. H., Johnson, M. (2009) Control of spin precession in a spin-injected field effect transistor. *Science* 325, 1515–1518

[9] Wunderlich, J. Park, B.-G., Irvine, A. C., Zârbo, L. P., Rozkotová, E., Nemec, P., Novák, V., Sinova, J., Jungwirth, T. (2010)Spin Hall effect transistor. *Science* 330, 1801–1804.
10 Tahara, T., Koike, H., Kameno, M., Sasaki, T., Ando, Y., Tanaka, K., Miwa, S., Suzuki, Y., and Shiraishi, M. (2015) Room-temperature operation of Si spin MOSFET with high on/off spin signal ratio. *Appl. Phys. Express* 8, 113004.
[11] Dash, S. P., Sharma, S., Patel, R. S., de Jong, M. P., & Jansen, R. (2009). Electrical creation of spin polarization in silicon at room temperature. *Nature*, *462*(7272), 491.
[12] Sharma, S., Spiesser, A., Dash, S. P., Iba, S., Watanabe, S., van Wees, B. J., Saito, H., Yuasa, S. & Jansen, R. (2014). Anomalous scaling of spin accumulation in ferromagnetic tunnel devices with silicon and germanium. *Physical Review B*, *89*(7), 075301.
[13] Fischer, I. A., Chang, L. T., Sürgers, C., Rolseth, E., Reiter, S., Stefanov, S., Chiussi, S., Tang, J., Wang, K. L. & Schulze, J. (2014). Hanle-effect measurements of spin injection from Mn*5*Ge*3*C*0.8*/Al*2*O*3*-contacts into degenerately doped Ge channels on Si. *Applied Physics Letters*, *105*(22), 222408.
[14] Iba, S., Saito, H., Spiesser, A., Watanabe, S., Jansen, R., Yuasa, S., & Ando, K. (2012). Spin accumulation and spin lifetime in p-type germanium at room temperature. *Applied Physics Express*, *5*(5), 053004.
[15] Tran, M., Jaffrès, H., Deranlot, C., George, J. M., Fert, A., Miard, A., & Lemaître, A. (2009). Enhancement of the spin accumulation at the interface between a spin-polarized tunnel junction and a semiconductor. *Physical review letters*, *102*(3), 036601.
[16] Misuraca, J., Kim, J. I., Lu, J., Meng, K., Chen, L., Yu, X., Zhao, J., Xiong, P. & von Molnár, S. (2014). Bias current dependence of the spin lifetime in insulating Al*0.3*Ga*0.7*As. *Applied Physics Letters*, *104*(8), 082405.
[17] Jahangir, S., Doğan, F., Kum, H., Manchon, A., & Bhattacharya, P. (2012). Spin diffusion in bulk GaN measured with MnAs spin injector. *Physical Review B*, *86*(3), 035315.
[18] Han, W., Jiang, X., Kajdos, A., Yang, S. H., Stemmer, S., & Parkin, S. S. (2013). Spin injection and detection in lanthanum-and niobium-doped SrTiO*3* using the Hanle technique. Nature communications, 4, 2134.
[19] Fujita, Y., Yamada, S., Ando, Y., Sawano, K., Itoh, H., Miyao, M., & Hamaya, K. (2013). Room-temperature sign reversed spin accumulation signals in silicon-based devices using an atomically smooth Fe*3*Si/Si (111) contact. *Journal of Applied Physics*, *113*(1), 013916.
[20] Kawano, M., Santo, K., Ikawa, M., Yamada, S., Kanashima, T., & Hamaya, K. (2016). Spin transport in p-Ge through a vertically stacked Ge/Fe3Si junction. *Applied Physics Letters*, *109*(2), 022406.
[21] Kasahara, K., Fujita, Y., Yamada, S., Sawano, K., Miyao, M., & Hamaya, K. (2014). Greatly enhanced generation efficiency of pure spin currents in Ge using Heusler compound Co*2*FeSi electrodes. *Applied Physics Express*, *7*(3), 033002.
[22] Yamada, M., Tsukahara, M., Fujita, Y., Naito, T., Yamada, S., Sawano, K., & Hamaya, K. (2017). Room-temperature spin transport in n-Ge probed by four-terminal nonlocal measurements. *Applied Physics Express*, *10*(9), 093001.
[23] Yamada, S., Honda, S., Hirayama, J., Kawano, M., Santo, K., Tanikawa, K., Kanashima, T., Itoh, H. & Hamaya, K. (2016). Magnetic properties and interfacial characteristics of all-epitaxial Heusler-compound stacking structures. *Physical Review B*, *94*(9), 094435.
[24] Sakai, S., Kawano, M., Ikawa, M., Sato, H., Yamada, S., & Hamaya, K. (2017). Low-temperature growth of fully epitaxial CoFe/Ge/Fe*3*Si layers on Si for vertical-type semiconductor spintronic devices. *Semiconductor Science and Technology*, *32*(9), 094005.
[25] Dankert, A., Dulal, R. S., & Dash, S. P. (2013). Efficient spin injection into silicon and the role of the Schottky barrier. *Scientific reports*, *3*, 3196.
[26] Rortais, F., Vergnaud, C., Ducruet, C., Beigné, C., Marty, A., Attané, J. P., Widiez, J., Jaffrès, H., George, J.-M. & Jamet, M. (2016). Electrical spin injection in silicon and the role of defects. *Physical Review B*, *94*(17), 174426.

[27] Sasaki, T., Suzuki, T., Ando, Y., Koike, H., Oikawa, T., Suzuki, Y., & Shiraishi, M. (2014). Local magnetoresistance in Fe/MgO/Si lateral spin valve at room temperature. *Applied Physics Letters*, *104*(5), 052404.
[28] Varnakov, S. N., Lepeshev, A. A., Ovchinnikov, S. G., Parshin, A. S., Korshunov, M. M., & Nevoral, P. (2004). Automation of technological equipment for obtaining multilayer structures in an ultrahigh vacuum. *Instruments and Experimental Techniques*, *47*(6), 839-843.
[29] Yakovlev, I. A., Varnakov, S. N., Belyaev, B. A., Zharkov, S. M., Molokeev, M. S., Tarasov, I. A., & Ovchinnikov, S. G. (2014). Study of the structural and magnetic characteristics of epitaxial Fe3Si/Si (111) films. JETP letters, 99(9), 527-530.
[30] Tarasov, A. S., Lukyanenko, A. V., Tarasov, I. A., Bondarev, I. A., Smolyarova, T. E., Kosyrev, N. N., Komarov, V.A., Yakovlev, I.A., Volochaev, M.N., Solovyov, L.A., Shemukhin, A.A., Varnakov, S.N., Ovchinnikov, S.G., Patrin, G.S., & Volkov, N.V. (2017). Approach to form planar structures based on epitaxial Fe*1-x*Si*x* films grown on Si (111). *Thin Solid Films*, *642*, 20-24.
[31] Tarasov, I.A., Popov, Z. I., Varnakov, S. N., Molokeev, M. S., Fedorov, A. S., Yakovlev, I. A., Fedorov, D. A., Ovchinnikov, S. G. (2014). Optical Characteristics of an Epitaxial Fe_3Si/Si(111) Iron Silicide Film. *JETP Letters*, 99, 565.
[32] Oki, S., Yamada, S., Tanikawa, K., Yamasaki, K., Miyao, M., and Hamaya, K. (2013). Lateral spin valves with two-different Heusler-alloy electrodes on the same platform. *Appl. Phys. Lett.*, 103, 212402
[33] Tarasov, I., Popov, Z., Visotin, M., Yakovlev, I., Varnakov, S. (2018). Effect of chemical ordering on optical properties of Fe_3Si epitaxial films. *EPJ Web Conf.*, 185, 03014.
[34] Karel, J., Juraszek, J., Minar, J., Bordel, C., Stone, K. H., Zhang, Y. N., Hu, J., Wu, R. Q., Ebert, H., Kortright, J. B., & Hellman, F. (2015). Effect of chemical order on the magnetic and electronic properties of epitaxial off-stoichiometry Fe*x*Si*1−x* thin films. *Physical Review B*, *91*(14), 144402.
[35] Wang, K., & Smith, A. R. (2011). Efficient kinematical simulation of reflection high-energy electron diffraction streak patterns for crystal surfaces. *Computer Physics Communications*, *182*(10), 2208-2212.
[36] Sandalov, I., Zamkova, N., Zhandun, V., Tarasov, I., Varnakov, S., Yakovlev, I., Solovyov, L., and Ovchinnikov, S. (2015). Effect of electron correlations on the Fe*3*Si and α−FeSi*2* band structure and optical properties. *Physical Review B*, 92, 205129.
[37] Hines, W. A., Menotti, A. H., Budnick, J. I., Burch, T. J., Litrenta, T., Niculescu, V., & Raj, K. (1976). Magnetization studies of binary and ternary alloys based on Fe*3*Si. *Physical Review B*, *13*(9), 4060.
[38] Yamada, S., Sagar, J., Honda, S., Lari, L., Takemoto, G., Itoh, H., Hirohata, A., Mibu, K., Miyao, M., & Hamaya, K. (2012). Room-temperature structural ordering of a Heusler compound Fe*3*Si. *Physical Review B*, *86*(17), 174406.
[39] Lenz, K., Kosubek, E., Baberschke, K., Wende, H., Herfort, J., Schönherr, H. P., & Ploog, K. H. (2005). Magnetic properties of Fe*3*Si*/* GaAs (001) hybrid structures. *Physical Review B*, *72*(14), 144411.
[40] Herfort, J., Schönherr, H. P., & Ploog, K. H. (2003). Epitaxial growth of Fe*3*Si/GaAs (001) hybrid structures. *Applied physics letters*, *83*(19), 3912-3914.
[41] Volkov, N. V., Tarasov, A. S., Eremin, E. V., Eremin, A. V., Varnakov, S. N., & Ovchinnikov, S. G. (2012). Frequency-dependent magnetotransport phenomena in a hybrid Fe/SiO*2*/p-Si structure. *Journal of Applied Physics*, *112*(12), 123906.
[42] Volkov, N. V., Tarasov, A. S., Smolyakov, D. A., Gustaitsev, A. O., Rautskii, M. V., Lukyanenko, A. V., Volochaev, M. N., Varnakov, S. N., Yakovlev, I. A., & Ovchinnikov, S. G. (2017). Extremely high magnetic-field sensitivity of charge transport in the Mn/SiO*2*/p-Si hybrid structure. *AIP Advances*, *7*(1), 015206.

[43] Dash, S. P., Sharma, S., Le Breton, J.C., Peiro, J., Jaffrès, H., George, J.-M., Lemaître, A., & Jansen, R. (2011). Spin precession and inverted Hanle effect in a semiconductor near a finite-roughness ferromagnetic interface. *Phys. Rev. B*, *84*, 054410.
[44] K. Hamaya, Y. Baba, G. Takemoto, K. Kasahara, S. Yamada, K. Sawano, and M. Miyao. Qualitative study of temperature-dependent spin signals in n-Ge-based lateral devices with Fe*3*Si/n-Ge Schottky-tunnel contacts. *Journal of Applied Physics* 113, 183713 (2013)
[45] Ishikawa, M., Oka, T., Fujita, Y., Sugiyama, H., Saito, Y., & Hamaya, K. (2017). Spin relaxation through lateral spin transport in heavily doped n-type silicon. *Physical Review B*, *95*(11), 115302.
[46] Sze, S. M., & Ng, K. K. (2006). *Physics of semiconductor devices*. John wiley & sons, p. 30, p. 26
[47] Spiesser, A., Sharma, S., Saito, H., Jansen, R., Yuasa, S., & Ando, K. (2012, October). Electrical spin injection in p-type Si using Fe/MgO contacts. *In Spintronics* V (Vol. 8461, p. 84610K). *International Society for Optics and Photonics.*
[48] Fert, A., & Jaffres, H. (2001). Conditions for efficient spin injection from a ferromagnetic metal into a semiconductor. *Physical Review B*, *64*(18), 184420.
[49] Cheung, S. K., & Cheung, N. W. (1986). Extraction of Schottky diode parameters from forward current-voltage characteristics. *Applied Physics Letters*, *49*(2), 85-87.
[50] Sze, S. M., & Ng, K. K. (2006). *Physics of semiconductor devices*. John wiley & sons, p. 84.
[51] Jansen, R., Deac, A. M., Saito, H., & Yuasa, S. (2012). Injection and detection of spin in a semiconductor by tunneling via interface states. *Physical Review B*, *85*(13), 134420.
[52] Losee, D. L. (1975). Admittance spectroscopy of impurity levels in Schottky barriers. *Journal of Applied Physics*, *46*(5), 2204-2214.
[53] Dueñas, S., Izpura, I., Arias, J., Enriquez, L., & Barbolla, J. (1991). Characterization of the DX centers in AlGaAs: Si by admittance spectroscopy. *Journal of applied physics*, *69*(8), 4300-4305.
[54] Volkov, N. V., Tarasov, A. S., Smolyakov, D. A., Gustaitsev, A. O., Balashev, V. V., & Korobtsov, V. V. (2014). The bias-controlled giant magnetoimpedance effect caused by the interface states in a metal-insulator-semiconductor structure with the Schottky barrier. *Applied Physics Letters*, *104*(22), 222406.
[55] Kudrnovský, J., Christensen, N. E., & Andersen, O. K. (1991). Electronic structures and magnetic moments of Fe*3*+ *y*Si*1*− *y* and Fe*3*−*x*V*x*Si alloys with DO3-derived structure. *Physical Review B*, *43*(7), 5924.
[56] Zamkova, N. G., Zhandun, V. S., Ovchinnikov, S. G., & Sandalov, I. S. (2017). Effect of local environment on moment formation in iron silicides. *Journal of Alloys and Compounds*, *695*, 1213-1222.